



In-Plane Semi-Linear Cloaks with Arbitrary Shape

Dengke Guo¹ Zheng Chang^{2*} Gengkai Hu¹

(¹Key Laboratory of Dynamics and Control of Flight Vehicle, Ministry of Education, School of Aerospace Engineering, Beijing Institute of Technology, Beijing 100081, China)

(²College of Science, China Agricultural University, Beijing 100083, China)

Received 27 November 2018; revision received 8 April 2019; Accepted 9 April 2019;
published online 17 April 2019

© The Chinese Society of Theoretical and Applied Mechanics 2019

ABSTRACT Soft materials with semi-linear strain energy function can be used as smart transformation media to manipulate elastic waves via finite pre-deformation. However, the intrinsic constraints involved in such materials limit the shapes of transformation devices to very simple cases. In this work, combining theoretical and numerical analyses, we report an approach of achieving the in-plane elastodynamic cloak with arbitrary shape. We demonstrate that with the appropriate out-of-plane stretch applied on the semi-linear material, cloaking effect can be achieved for both P- and SV-waves in the symmetric plane of a 3D domain, and the performance of the cloak with arbitrary cross section can be guaranteed for relatively small in-plane rotation. In addition, we propose an empirical formula to predict the deformation limit of the cloaks with semi-linear materials. This work may stimulate the experimental research on soft-matter-based transformation devices. Potential applications can be anticipated in nondestructive testing, structure impact protection, biomedical imaging and soft robotics.

KEY WORDS Elastic waves, Cloak, Hyperelasticity, Semi-linear, Arbitrary shape

1. Introduction

The transformation method, proposed by Pendry et al. [1] and Leonhardt [2] in electromagnetics, has become a powerful tool for the manipulation of wave fields and has drawn considerable attention in different realms of physics [3, 4]. In elastodynamics, such a technique possesses a great potential for applications in many branches of engineering, such as nondestructive testing, structure impact protection and seismology. The most fascinating paradigm of the transformation method, the invisibility cloak [5–7], has been extensively researched. However, in contrast to the fact that various cloaking devices have been demonstrated in electromagnetics [5] and acoustics [8, 9], the experimental work pertinent to elastodynamic cloaking has been seldom reported. As the elastodynamic transformation theory has been well established [7, 10], the major challenge for the realization of an elastodynamic cloak focuses on the design and fabrication of materials with complex properties in a broad frequency range. Although much effort has been directed toward the elastodynamic metamaterial technique, and the materials with exotic properties such as negative mass density [11], anisotropic mass density [12], double negative [13] and dual anisotropy [14] have been fabricated, it is still difficult to meet the harsh requirement involved in the elastic cloak design.

* Corresponding author. E-mail: changzh@cau.edu.cn

Recently, the hyperelastic transformation method [15] has been proposed, which offers a new approach to addressing the aforementioned issue. In the theory, it reveals that pre-deformed hyperelastic materials with certain strain energy functions can possess space invariance and thus behave like smart transformation media in elastic wave controls. Without the requirement of microstructure-based material, the hyperelastic transformation method exhibits remarkable potential for non-dispersion and broadband wave manipulation. In addition, as a soft-material-based method, it has a natural advantage of integration with other soft systems and can be expected to find technologically significant applications in biomedical imaging and soft robotics.

In the traditional transformation method [16], the design approach includes two main steps. In the first step, the necessary material distribution is determined by a spatial mapping (or a coordinate transformation). In the second step, the material distribution is realized with metamaterial. As long as these two steps are mutually independent, and the mappings which bridge the space and the material are non-unique, there is sufficient flexibility to design the material properties [17, 18], device configuration [19] or the combination of both [20] by a purpose selection of the mapping function. However, similar flexibility ceases to exist in the hyperelastic transformation method due to the unique mapping governed by the equilibrium equation of finite deformation. As a consequence, both the wave control capacity and the shape of hyperelastic transformation device are limited to very simple cases. Previous studies [21–23] have demonstrated that neo-Hookean material can be used to manipulate S-waves. However, its incapability of controlling the P-waves makes it non-ideal for the construction of hyperelastic cloak, as significant scattering from the inner boundary of the cloak may be expected. On the other hand, the semi-linear material [15] was considered more promising for controlling both P- and S-waves. However, it shows that only the P-waves can be accurately manipulated, unless additional constraints are imposed on the principal stretch [15, 24]. Furthermore, in the design of cloaking devices using the semi-linear material, the gradient of pre-deformation is required to be symmetric [15], which can only be achieved with very few specific geometric configurations and load conditions. In this context, open questions include how to achieve the cloaking effect for both P- and S-waves in accordance with the hyperelastic transformation method and whether it is possible to design cloaking devices with arbitrary shape.

In this work, we propose an approach to construct the semi-linear cloak for in-plane elastic waves. We demonstrate that with appropriate in-plane and vertical pre-deformation applied on a domain of a semi-linear material, cloak effect can be achieved in the symmetric plane of the deformation field. In addition, we also illustrate that the cloak with arbitrary shape works in an efficient manner when the in-plane rotation is relatively small. Besides, we propose an empirical formula to predict the deformation capability of achieving semi-linear cloaks.

The paper is arranged as follows. Some theoretical backgrounds, including the hyperelastic transformation method and the semi-linear strain energy function, are briefly reviewed in Sect. 2. The approach to construct the in-plane semi-linear cloaks with regular and irregular shapes, together with the way in which to predict the deformation limit of the cloaking devices, is provided in Sect. 3. Moreover, the numerical simulations are illustrated in Sect. 4. A discussion on our results and on the avenues for future work is provided in Sect. 5.

2. Theoretical Backgrounds

2.1. Hyperelastic Transformation Method

Consider a stress-free hyperelastic domain Ω_0 which finitely deforms to the current configuration Ω , as illustrated in Fig. 1. With the deformation being represented by a mapping which maps any point \mathbf{X} in Ω_0 to a point \mathbf{x} in Ω as $\mathbf{x} = \mathbf{x}(\mathbf{X})$, $\forall \mathbf{X} \in \Omega_0$, the equilibrium equation can be written as

$$\nabla_i (A_{0ijkl} \nabla_k U_l) = 0 \quad (1)$$

in which U_i denotes the finite displacement, and

$$A_{0ijkl} = \frac{\partial^2 W}{\partial F_{ji} \partial F_{lk}} \quad (2)$$

is the elastic tensor expressed in the initial configuration. In Eq. (2), W denotes the strain energy function of the hyperelastic material and $F_{ij} = \partial x_i / \partial X_j$ is the deformation gradient.

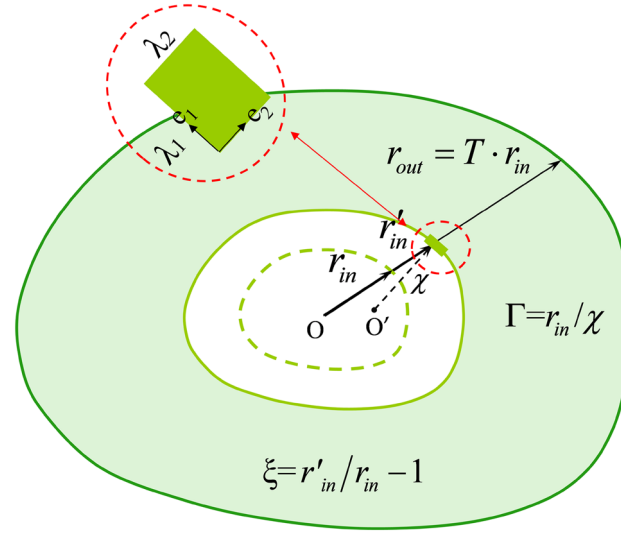


Fig. 1. Schematic diagram of an in-plane cloak. The outer boundary and the inner boundary before (the dashed line) and after (the solid line) a finite pre-deformation are similar and concentric to each other. The green rectangle represents an infinitesimal element on the inner boundary. Resulting from the deformation, any infinitesimal elements on the inner boundary are stretched in its principal directions e_1 and e_2 by factors λ_1 and λ_2 , respectively. The element can be identified with the dimensionless curvature $\Gamma = r_{in}/\chi$. (Color figure online)

In the framework of small-on-large theory [25], the incremental elastic wave motion u_i superposed on the deformed configuration Ω is governed by:

$$\nabla_i (A_{ijkl} \nabla_k u_l) = \rho \ddot{u}_j \quad (3)$$

in which A_{ijkl} and ρ denote the elastic tensor and mass density which are pushed forward to the current configuration, i.e.,

$$A_{ijkl} = J^{-1} F_{k\alpha} F_{l\beta} A_{0i\alpha j\beta} \quad (4)$$

$$\rho = J^{-1} \rho_0 \quad (5)$$

It has been noticed that the combination of Eqs. (4) and (5) has the same form as the asymmetric transformation relation [7, 26] in the elastodynamic transformation method. Therefore, to make an analogy between the small-on-large theory and asymmetric transformation elastodynamics, A_{0ijkl} is required to be equal to the stiffness of the un-deformed material, i.e.,

$$A_{0ijkl} = \lambda_0 \delta_{ij} \delta_{kl} + \mu_0 \delta_{ik} \delta_{jl} + \mu_0 \delta_{il} \delta_{kj} \quad (6)$$

in which λ_0 and μ_0 are the initial Lamé constants. Equation (6) plays a vital role in the hyperelastic transformation method, since an accurate manipulation of elastic waves can be achieved if and only if this condition is satisfied.

2.2. Semi-Linear Strain Energy Function

The isotropic semi-linear strain energy function can be written as [15]:

$$W_{\text{semi}} = \frac{\lambda_0}{2} (\text{tr} \mathbf{E})^2 + \mu_0 \text{tr} (\mathbf{E})^2 \quad (7)$$

in which $\mathbf{E} = \mathbf{U} - \mathbf{I}$ with $\mathbf{U} = \sqrt{\mathbf{F}^T \mathbf{F}}$ the right stretch tensor and \mathbf{I} the unit matrix.

Inserting Eq. (7) into Eq. (2), the second derivative of the strain energy function can be obtained and the local tangent modulus of the material is given by [24]

$$A_{0mjnl} = \lambda_0 R_{jm} R_{ln} + 2\mu_0 \delta_{lj} \delta_{mn} + (\lambda_0 U_{kk} - \lambda_0 \delta_{kk} - 2\mu_0) \frac{\partial R_{ln}}{\partial F_{jm}} \quad (8)$$

in which $\mathbf{R} = \mathbf{F}\mathbf{U}^{-1}$ is the rotation tensor. It is obvious that Eq. (6) does not hold for a general deformation gradient \mathbf{F} . Therefore, to utilize the hyperelastic transformation method with semi-linear material, some constraints have to be added to the deformation. In previous studies [15, 24], a special deformation mode has been proposed to realize in-plane wave (P-wave and SV-wave) control, which would be a good start point for the construction of semi-linear cloaks with arbitrary shape.

3. In-Plane Semi-Linear Cloaks

In this section, we will discuss about how to construct an in-plane cloak with proper pre-deformation, and propose an approach to predict the deformation limit to achieve cloaking devices. For simplicity, the shapes of the outer boundary and the inner boundary before and after the finite pre-deformation are considered similar and concentric to each other, as the schematic diagram shown in Fig. 1.

3.1. Conditions for In-Plane Semi-Linear Cloak

In Eq. (8), by specifying the deformation gradient as a symmetric one with $F_{13} = F_{23} = 0$, $F_{33} \neq 0$, the in-plane components of the elastic tensor can be obtained as

$$A_{\alpha\beta\gamma\rho}|_{\mathbf{F}=\mathbf{F}^T} = \lambda_0\delta_{\beta\alpha}\delta_{\rho\gamma} + 2\mu_0\delta_{\rho\beta}\delta_{\alpha\gamma} + (\lambda_0(U_{\eta\eta} - 3) - 2\mu_0)\frac{1}{F_{\eta\eta}}\varepsilon_{\beta\alpha}\varepsilon_{\rho\gamma} \quad (9)$$

in which all the indices $\alpha, \beta, \gamma, \rho$ and η range from 1 to 2 and $\varepsilon_{\beta\alpha}$ is the 2D permutation tensor. In this fashion, if the out-of-plane stretch is constrained with the in-plane deformation as

$$U_{33} = 1 - \frac{\lambda_0 + \mu_0}{\lambda_0}(U_{\eta\eta} - 2) \quad (10)$$

the condition of Eq. (6) is shown to be satisfied by substituting Eq. (10) into Eq. (9), and noting $U_{\eta\eta} = F_{\eta\eta}$. This reveals that the in-plane elastodynamic cloaking can be realized with the following two conditions.

- (i) The deformation gradient is symmetric with $F_{13} = F_{23} = 0$;
- (ii) The out-of-plane component (F_{33}) of the deformation gradient satisfies Eq. (10).

However, transformation devices usually require inhomogeneous in-plane deformation. This will make $U_{\eta\eta} = \lambda_1 + \lambda_2$ vary by location. As a result, the out-of-plane stretch $U_{33} = \lambda_3$ has to be non-uniform, and F_{13} and F_{23} have to be nonzero in the 3D semi-linear domain, which violates condition (i). To address this issue, we propose to apply symmetrical deformation in the out-of-plane direction, e.g., the tension or compression which is non-uniform in the considered 2D domain. In this case, the central plane becomes the symmetrical plane of the pre-deformation. F_{13} and F_{23} will become zero in such a plane, where the cloak effect can be anticipated.

3.2. In-Plane Semi-Linear Cloak with Arbitrary Shape

For the cloaks with irregular shape, the symmetric in-plane deformation can hardly be satisfied, and the nonzero rotation field has to be taken into account. Nevertheless, regardless of the violation of condition (i), we directly release the constraint on the symmetry of the in-plane deformation and consider the approximation of the arbitrary cloaks. As the rotation tensor can be expressed as $\mathbf{R} = [\cos \varphi, -\sin \varphi; \sin \varphi, \cos \varphi]$ with φ the rotation angle of an infinitesimal element, the deviation of the components of $A_{0m jnl}$ from those of the isotropic form [the right side of Eq. (6)] can be evaluated by Eq. (8). As an example, with the dimensionless initial material parameters set to be $\lambda_0 = 2$ and $\mu_0 = 1$, and \mathbf{U} set to be the unit tensor, the in-plane components A_{01121} and A_{01221} are plotted as functions of φ in Fig. 2. With φ varying from 0° to 60° , A_{01121} becomes nonzero, and A_{01221} gradually decreases. When φ reaches 26° , which corresponds to the maximal rotation in the semi-linear cloak proposed in Sect. 4, A_{01221} decreases by about 40%, as shown in Fig. 2. Since the rotation field in cloaking devices is inhomogeneous and mainly distributes along the inner boundary, we cannot explicitly figure out its influence on wave manipulation. However, through the numerical simulations in Sect. 4.1, we will demonstrate that the rotation field with such a level can be omitted, and condition (i) is approximately satisfied.

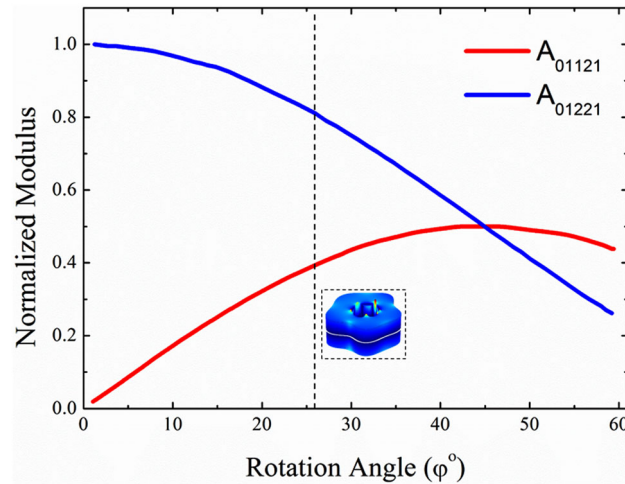


Fig. 2. Components A_{01121} and A_{01221} of the dimensionless elastic tensor of the infinitesimal element varying with the rotation angle $\varphi \in [0^\circ, 60^\circ]$ of the pre-deformation. In this case, the dimensionless initial material parameters are $\lambda_0 = 2$ and $\mu_0 = 1$, respectively, and the principal stretches are $\lambda_1 = \lambda_2 = 1$. The dashed line denotes the maximum rotation angle (26°) in the semi-linear cloak proposed in Sect. 4.1

3.3. Deformation Limit of the Cloaks

For a semi-linear cloak, it is of interest to consider the maximum pre-deformation allowed to construct the cloak, since it reflects the optimal stealth performance. In the hyperelastic transformation method, the physical deformation of semi-linear material limits the mapping to be one-to-one correspondent, and any unphysical “overlapping” or “folding” of infinitesimal elements is forbidden. In other words, in cloak design, it requires that:

- (iii) The principal stretches must be greater than zero during pre-deformation.

With this criterion, the upper deformation limit of semi-linear cloaks can be examined by the numerical scheme proposed in Sect. 4. In the following, we propose an empirical formula to predict this deformation limit, which will be compared with numerical simulations.

Due to the concentration of strain, the critical point of a semi-linear cloak can be found at the inner boundary, where the dimensionless curvature $\Gamma = r_{\text{in}}/\chi$ is maximum. In $\Gamma = r_{\text{in}}/\chi$, r_{in} is the initial distance from an infinitesimal element on the inner boundary to the centroid and χ is the local curvature of the boundary, as shown in Fig. 1. The deformation limit can be determined by the ultimate expansion ratio $\xi_{\text{max}} = r'_{\text{in}}/r_{\text{in}} - 1$ at the critical point, in which r'_{in} is the maximum distance from the infinitesimal element to the centroid in the deformed configuration.

For an elliptical cylindrical cloak, the dimensionless curvature on the inner boundary is monotonic, and the critical points constantly locate at the two vertexes. Therefore, by numerically calculating the ultimate expansion ratio of elliptical cylindrical cloaks with different outer/inner ratios T (see Fig. 1) and aspect ratios (or in other words, with different maximal dimensionless curvatures), we can establish a one-to-one correspondence between the maximal expansion ratio and the dimensionless curvature, as shown in Fig. 3. When T is relatively large, the constraint of the outer boundary can be ignored, and ξ_{max} can be approximated by the following relation,

$$\xi_{\text{max}} \approx 1 - 0.55 \lg \Gamma \quad (11)$$

as illustrated in Fig. 3. It also indicates that the cylindrical cloak ($\Gamma = 1$) allows the maximum ultimate expansion ratio ($\xi_{\text{max}} = 1$).

Equation (11) can be used as a reference to predict the deformation limit of a 2D cloak with arbitrary cross section, as long as the maximal dimensionless curvature can be determined. The effectiveness of such a procedure is validated through the arbitrary cloak proposed in Sect. 4.1. For that cloak, the maximum dimensionless curvature on the inner boundary is $\Gamma = 4$ at $\theta = \pi$; therefore, the ultimate

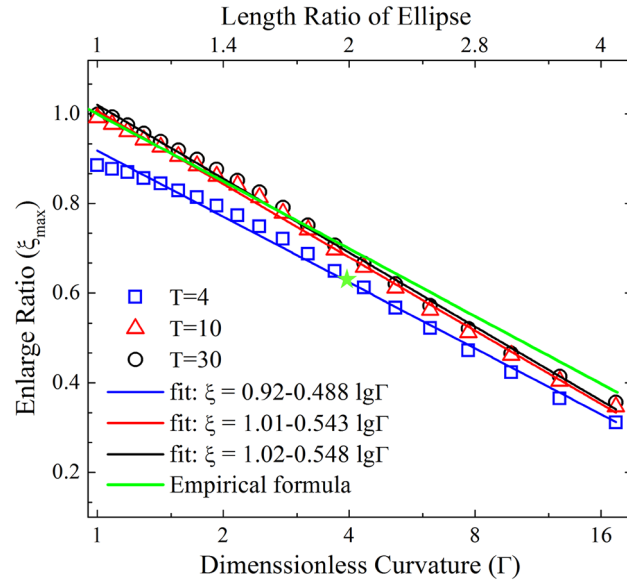


Fig. 3. The ultimate expansion ratios ξ_{\max} of cloaking devices as functions of dimensionless curvature Γ for different outer/inner ratios T . The symbols are numerical results for elliptical semi-linear cloaks with different aspect ratios (top label), whereas the lines are the corresponding fitting functions. The green line denotes the empirical formula for predicting the ultimate expansion ratio of an arbitrary cloak. The star denotes the deformation capability of the semi-linear cloak proposed in Sect. 4.1, which is obtained from numerical simulation. (Color figure online)

expansion ratio obtained from Eq. (11) is $\xi_{\max} = 0.65$, which agrees well with the numerical simulation ($\xi_{\max} = 0.65$), as illustrated in Fig. 3. It is worth noting that the deformation limit provided by Eq. (11) is an upper one. In practice, to avoid the device failure due to material instability and fracture, a safety factor should be considered in estimating the allowable deformation.

4. Numerical Simulations

Three steps are required for the simulation of the proposed cloak: in-plane deformation construction, 3D deformation construction and wave behavior analysis. All of them can be accomplished together using the COMSOL Multiphysics software.

In Step I, the in-plane deformation of a cloak can be obtained by solving a 2D static problem governed by Eq. (1). With the outer boundary fixed, the Dirichlet boundary condition $U(\theta) = \xi r_{\text{in}}$ is imposed on the inner boundary, in which ξ is the actual expansion ratio. By utilizing the structure mechanics module of COMSOL, the semi-linear strain energy function is imported as a user-defined material. In the static solver, nonlinear geometry is considered to deal with the finite deformation. The accuracy of the numerical scheme has been validated by a comparison with the analytical result for a cylindrical cloak [15]. It is worth mentioning that the model can also be utilized to predict numerically the deformation limit of an arbitrary cloak. By incrementally sweeping the expansion ratio, the ultimate one can be obtained when the calculation automatically aborts for the violation of condition (iii).

In Step II, with information of the in-plane deformation being obtained, the out-of-plane stretch is calculated from Eq. (10). In 3D simulation, by keeping the boundary conditions of inner and outer boundaries the same as those in Step I, the out-of-plane stretch can be accomplished by imposing body displacement load on the initial configuration. As aforementioned, the displacement should be symmetrical with respect to the out-of-plane direction. In this sense, the cloak region can be generated in the symmetrical plane of the deformed configuration.

In Step III, with A_0 and ρ in the symmetrical plane obtained from Step II, the in-plane cloak effect can be validated by solving a 2D problem governed by Eq. (3). The weak form PDE module of COMSOL is utilized to deal with the asymmetric elastic tensor. In modeling, the cloak is embedded in a reference medium with the same material parameters as the un-deformed semi-linear material. The perfectly matched layer technique [27] is employed to absorb the reflection from the model boundary.

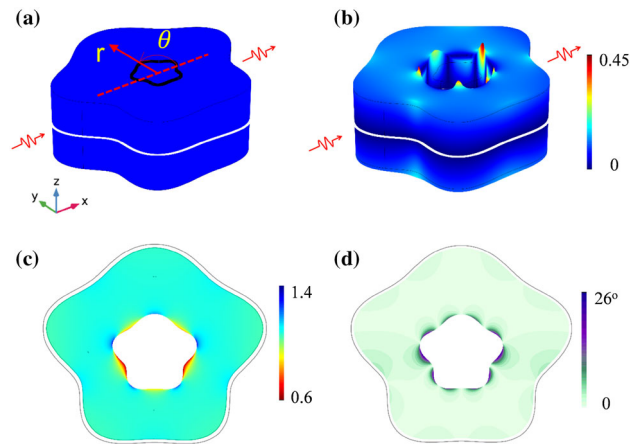


Fig. 4. Semi-linear cloak with arbitrary shape. **a** Cloak domain before pre-deformation, **b** total displacement field of the cloak after finite pre-deformation. The white curve denotes the symmetrical plane where the cloak can be anticipated, **c** distribution of the out-of-plane stretch in the symmetrical plane, **d** field of the rotation angle φ in the symmetrical plane

A small circle is placed outside the cloak as a point source, which, in turn, emits harmonic P- and SV-waves, respectively.

In the following, two numerical examples, a 2D barrel cloak with arbitrary cross section and a carpet cloak, are designed to demonstrate the effectiveness of the proposed scheme.

4.1. In-Plane Columnar Barrel Cloak with Arbitrary Cross Section

We consider a columnar semi-linear domain with the height of $h = 5$ m, and the initial cross section can be expressed by $f(\theta) = 50 + 5\sin\theta + 2\sin(3\theta) + 5\sin(5\theta) + \sin(7\theta)$, where θ is the azimuth, as shown in Fig. 4a. The inner and outer boundaries of the cloak region are $r_{\text{in}} = 0.03f(\theta)$ m and $r_{\text{out}} = 0.12f(\theta)$ m, respectively. Thus, the inner/outer ratio is $T = 4$. The dimensionless initial material parameters are considered to be $\lambda_0 = 2$, $\mu_0 = 1$ and $\rho = 1$. Within the deformation limit ($\xi_{\text{max}} = 0.67$) predicted by Eq. (11), we choose the actual expansion ratio to be $\xi = 0.55$. The deformed configuration of the cloak is shown in Fig. 4b. In the symmetrical plane (denoted by the white curve in Fig. 4b), the out-of-plane stretch (Fig. 4c) conforms with Eq. (10), and $F_{13} = F_{23} = 0$, as expected. The distribution of the rotation angle φ is plotted in Fig. 4d, showing that the rotation mainly distributes along the inner boundary, with the maximum value of 26° .

Consider a point source of SV-wave with the frequency of 0.8 Hz, the in-plane wave fields with and without the cloaking device are illustrated in Fig. 5. As the cloak is enlarged from a small cavity with finite radius, it will scatter the incident SV-wave and stimulate the P-wave simultaneously. For ease of comparison, the total SV-wave field, reflected SV-wave field and reflected P-wave field are provided in Fig. 5, with indices (i)–(iii), respectively. In comparison with the uncloaked case (large cavity without cloak, Fig. 5c), it shows that when the large cavity is covered with the semi-linear cloak (Fig. 5a), the scattering is significantly reduced to almost the same level as that of the reference case (small cavity without cloak, Fig. 5b). The result also shows that such a rotation level in the semi-linear cloak has no significant impact on cloak effect. It is worth noting that similar cloak effect can also be observed in the case of P-wave incidence.

To validate the broadband feature of the proposed cloak, a series of calculations has been performed in the frequency range of 0.5–1.5 Hz. Consequently, the total scattering cross sections (TSCS) $E_{\text{sca}} = \int_L (I_x n_x + I_y n_y) dl$ for each case are calculated, in which $I_i = \sigma_{ij} v_j$ denotes the energy flux, v_j is the velocity and n_j is the unit normal to the integration boundary L enclosing the cloak region ($i = x, y$). The reductions in TSCS $\gamma = (E_c - E_s)/E_c$ for both P- and SV-wave incidences are plotted in Fig. 6, in which E_c represents the TSCS for the uncloaked case and E_s represents the TSCS for the cloaked or reference case. It shows that, over the large frequency range, the semi-linear cloak reduces 30% of the TSCS resulted from the large cavity and keeps TSCS the same level as that of the reference case.

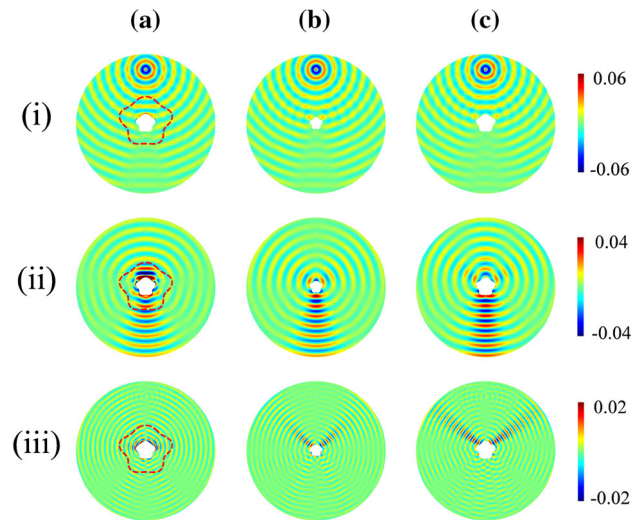


Fig. 5. In-plane wave fields in semi-linear material with and without the cloaking device due to an SV-wave point source. (a) cloaked case: large cavity with cloak, (b) reference case: small cavity without cloak, (c) uncloaked case: large cavity without cloak. (i) total SV-wave field, (ii) reflected SV-wave field, (iii) reflected P-wave field

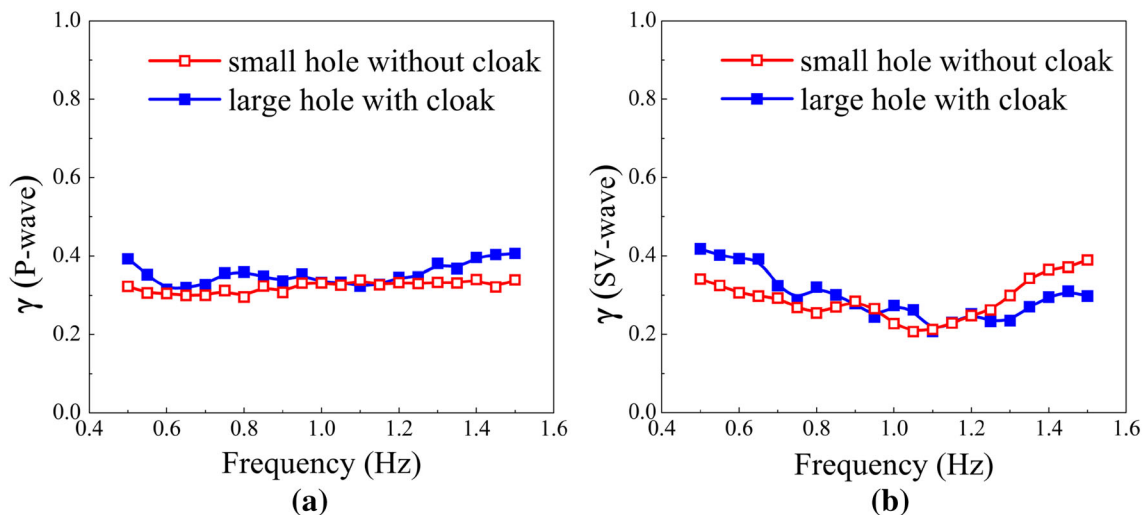


Fig. 6. Reduction in total scattering cross section γ of the semi-linear cloak (the blue curves) for frequency $f \in [0.5 \text{ Hz}, 1.5 \text{ Hz}]$. As a comparison, the red curves indicate γ in the reference case compared with the uncloaked case. **a** P-wave incidence, **b** SV-wave incidence. (Color figure online)

4.2. In-Plane Semi-Linear Carpet Cloak

With a similar procedure, an in-plane carpet cloak can also be constructed and validated. Consider a rectangular semi-linear domain of $8 \text{ m} \times 4 \text{ m} \times 5 \text{ m}$, with the material parameters identical to the previous example, as shown in Fig. 7a. The in-plane deformation can be obtained by curving one straight boundary and at the same time fixing the others. Resulting from the out-of-plane stretch, the deformed configuration of the semi-linear domain is provided in Fig. 7b. Again, in the symmetrical plane (the white curve in Fig. 7b), the out-of-plane stretch (Fig. 7c) conforms with Eq. (10), and $F_{13} = F_{23} = 0$ is satisfied. Besides, the rotation concentrates near the deformed boundary with a maximal rotation angle of 27° , as illustrated in Fig. 7d.

With the cloak embedded in an un-deformed semi-linear material with the same material properties, wave beams (the red dashed lines in Fig. 8) of P- and SV-modes are launched at an angle of 45° to the ground plane with the frequency of 4 Hz. The in-plane wave fields for the cases with and without

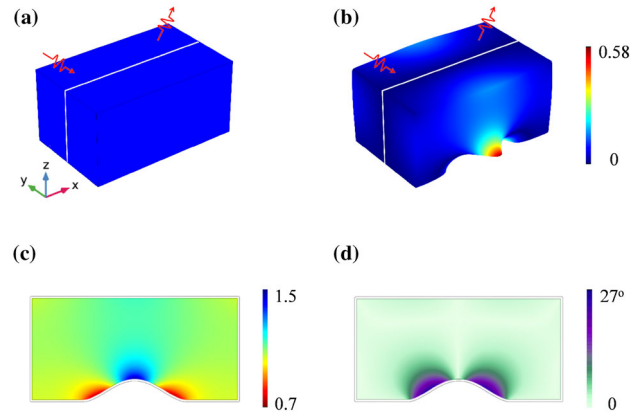


Fig. 7. Semi-linear carpet cloak. **a** Cloak domain before pre-deformation, **b** total displacement field of the cloak after finite pre-deformation. The white curve denotes the symmetrical plane; **c** distribution of the out-of-plane stretch in the symmetrical plane, **d** field of the rotation angle θ in the symmetrical plane

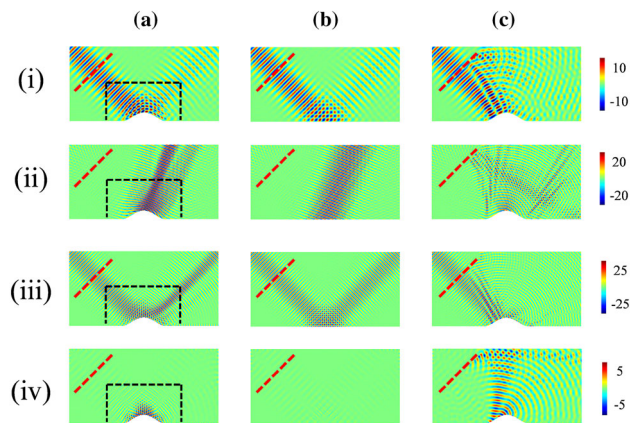


Fig. 8. In-plane wave fields in semi-linear material with and without the carpet cloak. (a) cloaked case: curved surface with the carpet cloak; (b) reference case: flat surface; (c) uncloaked case: curved surface without the carpet cloak. (i) total P-wave field, P-wave incidence, (ii) total SV-wave field, P-wave incidence, (iii) total P-wave field, SV-wave incidence, (iv) total SV-wave field, SV-wave incidence. (Color figure online)

the carpet cloak are shown in Fig. 8. For either P- or SV-wave incidence, the semi-linear carpet cloak (Fig. 8a) makes the elastic wave reflection and conversion in a similar manner as that of the flat ground case (Fig. 8b) and largely reduces the beam divergence of the curved ground (Fig. 8c).

5. Conclusions

Based on the hyperelastic transformation method, we have proposed an approach to construct in-plane elastic cloaks with semi-linear materials. By conducting both theoretical and numerical analyses, we have demonstrated that the broadband cloak effect can be achieved in the symmetric plane of a 3D semi-linear domain by incorporation with the external loads of in-plane displacement and out-of-plane stretch. We have found that the small in-plane rotation can be neglected in the cloak design, particularly with arbitrary cross section. We have also proposed an empirical formula with respect to the maximum dimensionless curvature to access the deformation limit to construct cloaking devices. In the next step, further effort will be directed toward the realization of the mechanical loading proposed in this work. It is a challenge as it requires that the loading devices do not affect wave propagation. In addition, it will be of great interest to design wave control devices with real semi-linear materials. We hope that this work may find some potential applications in such fields as nondestructive testing, structure impact protection, biomedical imaging and soft robotics.

Acknowledgements. The authors are grateful to Dr. Yi Chen for valuable discussions. This work was supported by the National Natural Science Foundation of China (Grant Nos. 11472044, 11521062, 11602294, 11632003) and the Chinese Universities Scientific Fund (Grant No. 2019TC134).

References

- [1] Pendry JB, Schurig D, Smith DR. Controlling electromagnetic fields. *Science*. 2006;312(5781):1780–2.
- [2] Leonhardt U. Optical conformal mapping. *Science*. 2006;312(5781):1777–80.
- [3] Chen T, Weng CN, Chen JS. Cloak for curvilinearly anisotropic media in conduction. *Appl Phys Lett*. 2008;93(11):114103.
- [4] Zhang S, Genov DA, Sun C, Zhang X. Cloaking of matter waves. *Phys Rev Lett*. 2008;100(12):123002.
- [5] Schurig D, Mock JJ, Justice BJ, Cummer SA, Pendry JB, Starr AF, Smith DR. Metamaterial electromagnetic cloak at microwave frequencies. *Science*. 2006;314(5801):977–80.
- [6] Norris AN. Acoustic cloaking theory. *Proc R Soc A Math Phys Eng Sci*. 2008;464(2097):2411.
- [7] Norris AN, Shuvalov AL. Elastic cloaking theory. *Wave Motion*. 2011;48(6):525–38.
- [8] Chen HY, Chan CT. Acoustic cloaking in three dimensions using acoustic metamaterials. *Appl Phys Lett*. 2007;91(18):183518.
- [9] Chen Y, Zheng MY, Liu XN, Bi YF, Sun ZY, Xiang P, Yang J, Hu GK. Broadband solid cloak for underwater acoustics. *Phys Rev B*. 2017;95(18):180104.
- [10] Hu J, Chang Z, Hu GK. Approximate method for controlling solid elastic waves by transformation media. *Phys Rev B*. 2011;84(20):201101.
- [11] Liu ZY, Zhang XX, Chan CT, Sheng P. Locally resonant sonic materials. *Science*. 2000;289(5485):1734–6.
- [12] Zhu R, Yasuda H, Huang GL, Yang JK. Kirigami-based elastic metamaterials with anisotropic mass density for subwavelength flexural wave control. *Sci Rep*. 2018;8(1):483.
- [13] Liu XN, Hu GK, Huang GL, Sun CT. An elastic metamaterial with simultaneously negative mass density and bulk modulus. *Appl Phys Lett*. 2011;98(25):251907.
- [14] Cheng Y, Zhou XM, Hu GK. Broadband dual-anisotropic solid metamaterials. *Sci Rep*. 2017;7(1):13197.
- [15] Norris AN, Parnell WJ. Hyperelastic cloaking theory: transformation elasticity with pre-stressed solids. *Proc R Soc A Math Phys Eng Sci*. 2012;468(2146):2881–903.
- [16] Chen HY, Chan CT, Sheng P. Transformation optics and metamaterials. *Nat Mater*. 2010;9:387.
- [17] Li J, Pendry JB. Hiding under the carpet: a new strategy for cloaking. *Phys Rev Lett*. 2008;101(20):203901.
- [18] Chang Z, Hu J, Hu GK. Controlling elastic waves with isotropic materials. *Appl Phys Lett*. 2011;98(12):121904.
- [19] Hu J, Zhou XM, Hu GK. Design method for electromagnetic cloak with arbitrary shapes based on Laplace's equation. *Opt Express*. 2009;17(15):13070.
- [20] Chang Z, Zhou XM, Hu J, Hu GK. Design method for quasi-isotropic transformation materials based on inverse Laplace's equation with sliding boundaries. *Opt Express*. 2010;18(6):6089–96.
- [21] Chang Z, Guo HY, Li B, Feng XQ. Disentangling longitudinal and shear elastic waves by neo-Hookean soft devices. *Appl Phys Lett*. 2015;106(16):161903.
- [22] Parnell WJ. Nonlinear pre-stress for cloaking from antiplane elastic waves. *Proc R Soc A Math Phys Eng Sci*. 2012;468(2138):563–80.
- [23] Parnell WJ, Norris AN, Shearer T. Employing pre-stress to generate finite cloaks for antiplane elastic waves. *Appl Phys Lett*. 2012;100(17):171907.
- [24] Guo DK, Chen Y, Chang Z, Hu GK. Longitudinal elastic wave control by pre-deforming semi-linear materials. *J Acoust Soc Am*. 2017;142(3):1229–35.
- [25] Ogden RW. Incremental statics and dynamics of pre-stressed elastic materials. In: Destrade M, Saccomandi G, editors. *Waves in nonlinear pre-stressed materials*. Vienna: Springer; 2007. p. 1–26.
- [26] Brun M, Guenneau S, Movchan AB. Achieving control of in-plane elastic waves. *Appl Phys Lett*. 2009;94(6):061903.
- [27] Chang Z, Guo DK, Feng XQ, Hu GK. A facile method to realize perfectly matched layers for elastic waves. *Wave Motion*. 2014;51(7):1170–8.